*Bangladesh Journal of Physics, **25**, 55-64, June 2019*

ALTERNATING CURRENT ELECTRICAL PROPERTIES OF CERIUM DOPED BARIUM TITANATE BELOW THE ROOM TEMPERATURE

MOHAMMAD JELLUR RAHMAN[1*], AFIA IFFAT[2], MD. ABU HASHAN BHUIYAN[1] AND SHAMIMA CHOUDHURY[2]

[1]*Department of Physics, Bangladesh University of Engineering and Technology, Dhaka-1000, Bangladesh*

[2]*Department of Physics, University of Dhaka, Dhaka-1000, Bangladesh*

Corresponding Author's Email: mjrahman@phy.buet.ac.bd

Received on 22.05.2019 Revised received on 26.08.2019, Accepted for publication on 27.08.2019

ABSTRACT

The alternating current (*ac*) electrical properties (dielectric constant, loss tangent and *ac* conductivity) of pure and cerium (Ce) doped barium titanate ($BaTiO_3$) with a general formula $Ba_{1-x}Ce_xTiO_3$ where x=0.00, 0.01, 0.02, 0.03 and 0.04 were studied at the temperature range −25to 30°C. The samples were prepared by the conventional solid state reaction method and sintered at 1200 °C for 4 hours. The structural properties of $BaTiO_3$ and Ce doped $BaTiO_3$ were also studied. The scanning electron microscope micrographs for different doping concentration of Ce showed increase in grain size with doping concentration. Lattice constant and particle size of the samples were observed to decrease slightly with Ce doping as obtained from the X-ray diffraction measurements. The dielectric constant of the sample increases with temperature and undergoes a transition from orthorhombic to tetragonal at about 270 K. The value of dielectric constant sharply decreases with frequency up to 1 kHz and beyond that remains almost stable for all the samples at different temperatures. Dielectric loss at different temperatures showed a good agreement with frequency. The *ac* conductivity, σ_{ac} of the samples increases with the increase in frequency reaches to a maximum value and then shows a decreasing trend. The frequencies of peak σ_{ac} are observed to be shifted towards lower frequency with the increase in doping content.

Keywords: Barium Titanate, Perovskite ceramics, Dielectric constant, *ac* electrical properties.

1. INTRODUCTION

Ferroelectric materials having high dielectric constant (ε') are of great interest since 1942 [1]. Barium Titanate ($BaTiO_3$) is one of the most widely used ferroelectric material, and even sixty years after its discovery it is still the most important multilayer ceramic dielectric. Owing to high ε' and electro-optics co-efficient of $BaTiO_3$ it has become more and more important in ceramics materials and therefore its dielectric characteristic become very important in the field of electronic industry and technology. $BaTiO_3$ ceramics has strong piezoelectric effect and are mechanically rugged and rather insensitive to temperature and humidity [2]. Primary application requisites are a high capacitance and stable capacitance over the temperature range of use of the component. Pure $BaTiO_3$ has a peak permittivity at about 130°C and another secondary peak at 10 °C while the practical temperature ranges from -55 to 125 °C or segments within that range [3]. As a semiconductor it exhibits positive temperature of co-efficient of resistivity (PTCR) in its

crystalline form. At a certain temperature, called the Curie temperature (T_c), the material exhibits an increase in resistivity typically being several orders of magnitude. At T_c, $BaTiO_3$ undergoes a phase change from tetrahedral to cubic above room temperature [2]. It has also been reported that single crystals of $BaTiO_3$ exhibit negative temperature co-efficient of resistivity (NTCR) properties and the T_c can be controlled by the dopant to some extent. Due to its PTCR properties $BaTiO_3$ is most often used as a thermistor e.g., in thermal switches. As being a pure crystalline, these ceramics has wide applications including micro-electro mechanical systems, multilayer ceramics capacitors, piezoelectric transducers, microwave devices and different type of storage information devices, infrared sensors, microphones, ultrasonic and underwater transducers, multilayer capacitors and spark generators [2].

The ferroelectric properties of this ABO_3 type perovskite ceramics can be controlled by doping with different elements. Various A and B site substitutions in different concentration has been tried to effect on it [4,5]. The T_c value observed to decrease linearly towards the room temperature on substituting Sr^{2+} to the A site while the substitution of Pb^{2+} for Ba^{2+} increases T_c. The simultaneous substitution with different ions into both A and B sites can be used to modify the characteristics of $BaTiO_3$[6]. Ce is chosen as $BaTiO_3$ ceramics with highly doped Ce have been described as having promising dielectric properties, such as high permittivity and high endurance and lot of advanced studies are being performed [7–9]. They can be used in the production of multilayer ceramics capacitors [10]. However, capacitor formulations based on $BaTiO_3$ need to be modified chemically and physically to produce the required capacitance temperature characteristics, which can be created by the resistance of Ce doped regions. Ce can exist in two excitation states (3^+ and 4^+), and can be substuted into the $BaTiO_3$ perovskite lattice in both existing oxidation states. In the excitation state 3^+ it is incorporated at Ba^{2+} sites and acts as donor, whereas in the 4^+ state it enters Ti^{4+} sites of the $BaTiO_3$ lattice. As donor Ce requires the formation of effectively negatively charged compensating lattice defects. The donor charge compensation mechanism and the sites where Ce enters the $BaTiO_3$ lattice depend on the firing atmosphere and on the starting composition [11,12].When $BaTiO_3$ is sintered in air together with CeO_2 and an excess amount of BaO, Ce is incorporated intoTi^{4+} sites. The solubility limit of $BaTi_{1-x}Ce_x^{4+}O_3$ solid solution is relatively high (x= 0.36at 1400 °C) [13-15]. However, when $BaTiO_3$ is sintered in air together with CeO_2 and an excess amount of TiO_2, CeO_2 is partially reduced and Ce enters into the $BaTiO_3$ lattice as a donor at the Ba sites. The excess charge in highly Ce^{3+} doped $BaTiO_3$ is compensated by the formation of ionized vacancies at Ti^{4+} sites [16]. The solubility limit of solid solution of $Ba_{1-x}Ce_x^{3+}TiO_3$ is highly temperature dependent (x = 0.04 at 1200°C and x = 0.08 at 1400 °C).

At the temperature in an atmosphere with a low oxygen partial pressure, CeO_2 is totally reduced and consequently Ce dissolved in $BaTiO_3$ in the oxidation state 3+, independently of the starting composition. In contrast to most of the rare-earth elements, which are stable in air in oxidation states 3+, Ce is the most stable in oxidation state 4+.Due to its high $\varepsilon'$and low loss characteristics, it has been used in applications, such as multilayer capacitors. Doped $BaTiO_3$ has found wide applications in semiconductors, PTC thermistors and piezoelectric devices. In comparison with other dielectric materials $BaTiO_3$ has some limitations. But these limitations must be eliminated to get the optimum results from its dielectric properties. $\varepsilon'$of $BaTiO_3$ depends on frequency and external electric field. The domain of $BaTiO_3$ is more effectively oriented at high electric field strength and results in higher dielectric constants, which sharply peaks at T_c and loss characteristics follow the same shape. ε'also strongly depends on temperature. By forming solid

solution over a wide range of compositions, T_c and ε'can be modified. T_c of ceramics also depends on particle and grain size. Ba/Ti ratio and sintering parameters play significant roles determining the grain size and density, and grain size affects the dielectric properties of the $BaTiO_3$ ceramics. As dielectric properties also depend on the ionic size and polarization, in this work the structural and morphological properties are studied for the Ce doped $BaTiO_3$ in the temperature range –25° C to 30° C for different doping (Ce) concentration and their effect on grain size is also studied. The main objective of this is to study the alternating current (*ac*) electrical properties i.e., dielectric constant, loss tangent and conductivity of $BaTiO_3$ below the room temperature.

2. EXPERIMENTAL DETAILS

Barium oxide (BaO), titanium dioxide (TiO_2) and cerium oxide (CeO_2) were used for the preparation of $Ba_{1-x}Ce_xTiO_3$samples (where x=0.00, 0.01, 0.02, 0.03 and 0.04) and the raw oxides were collected from the local market. The samples were prepared by solid state reaction method, where BaO and TiO_2 were used as the parent materials and CeO_2 was used as an additive. An appropriate amount of the starting materials were thoroughly mixed, dried and ball milled in a polyethylene jar for 12 hours in a wet medium and then calcined at 900 °C for three hours. The calcined powders were re-milled for 12 hours and pellets were formed by manually pressurizing the mixture. The pellets were then sintered at 1200 °C for four hours. A Philips PW3040 X'Pert PRO X-ray diffractometer were used to study the crystal structure of the samples using a monochromatic Cu-K_α radiation (λ=1.54053 Å) to ensure the formation of single-phase nature of the sintered product. A Hitachi S-3400N scanning electron microscope (SEM) was employed for the observation of the surface morphology and an estimation of grain sizes with increasing Ce content. These pellets were used for the measurement of the temperature-dependent resistivity and ε'. For the electrical measurements both sides of the samples were coated with highly-conducting silver paste (Demetron, Leipzigerstr. 10, Germany) after polishing. A two-probe method was used for the measurement of the resistance and capacitance of the samples. Measurements of dielectric properties (capacitance, loss tangent and ac conductivity) were performed by a low frequency impedance analyzer (Agilent 4192A, Agilent Technologies, Japan) in the frequency range 0.1 to 100 kHz.

3. RESULTS AND DISCUSSION

3.1 X-ray Diffraction Analysis

X-ray diffraction (XRD) spectra of $Ba_{1-x}Ce_xTiO_3$ samples where x = 0.0, 0.01, 0.02, 0.03 and 0.04 are shown in Fig. 1. The XRD spectrum shows mainly $BaTiO_3$ phase in the samples with a secondary phase of $BaTi_2O_5$ and thus solid state reaction is conjectured to be occurred when BaO, TiO_2 and CeO_2 were mixed according to the formula $Ba_{1-x}Ce_xTiO_3$ (where x = 0.00, 0.01, 0.02, 0.03 and 0.04) and sintered at 1200°C for 4 hours. The observed position of the diffraction peaks (100), (110), (111), (200), (210), (211) and (220) appear identical for all the samples and thus have confirmed all the studied samples with a very small amount of impurity phase detected with the manifestation of very weak peak intensity between (100) and (110) fundamental peaks. By changing the Ce doping concentration the positions of the diffraction peaks do not change significantly, which also indicates that the crystal structure remains unchanged. The positions of the diffraction peaks confirmed that all the studied samples are mainly of the $BaTiO_3$ phase with a small secondary phase of $BaTi_2O_5$. The diffraction peaks for the secondary phase may be due to

the preparation of samples using raw BaO, CeO_2 and TiO_2. Dopant Ce ions with a small radius may form the core-shell-structured fine grains and thus secondary phase may appear [17].

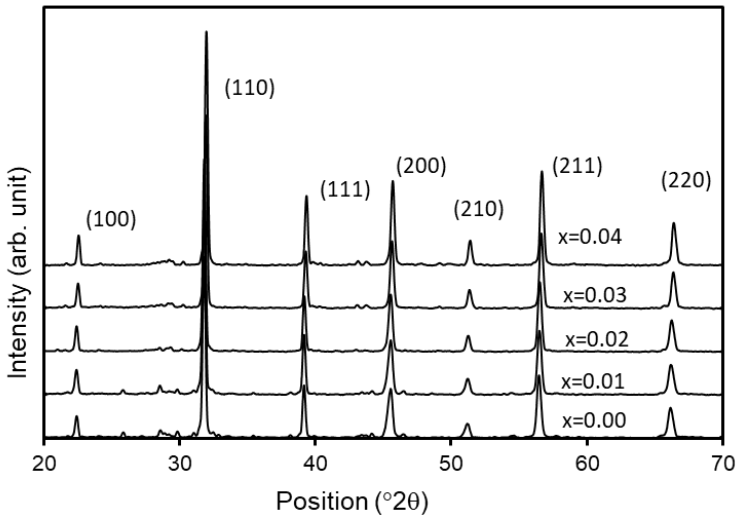

Fig.1. XRD patterns of the samples of $Ba_{1-x}Ce_xTiO_3$(where x=0.00, 0.01, 0.02, 0.03 and 0.04) compounds sintered at 1200 °C.

All the reflection peaks were indexed and the lattice parameters were determined by the Nelson-Riley(NR) method using the NR function, which is defined as

$$F(\theta) = \frac{1}{2}\left(\frac{\cos^2\theta}{\sin\theta} + \frac{\cos^2\theta}{\theta}\right), \quad \ldots \quad \ldots \quad \ldots \quad (1)$$

whereθ is the Bragg angle[18], the particle size, D was calculated using the Debye-Scherrer equation

$$D = \frac{0.9\lambda}{\beta cos\theta} \quad \ldots \quad \ldots \quad \ldots \quad \ldots \quad \ldots \quad \ldots \quad \ldots(2)$$

where 0.9 is the shape factor, λ is the x-ray wavelength, β is the line broadening at half the maximum intensity(FWHM) in radians and θ is the Bragg angle. The calcualted lattice constants(a) and D are presented in Table 1 and the value of a and the values of NR function $F(\theta)$ were plotted as shown in Fig. 2(a),where the y values at $F(\theta) = 0$ give the exact value of lattice constants. It is observed that lattice constants slightly decrease with the increase of Ce doping with a value of 4.0685Å for x=0.00 to 4.0301Å for x = 0.04, which can be interpreted due to smaller ionic radii of dopant Ce (1.14 Å) with higher ionic radii of substituted Ba (1.42 Å)[18].

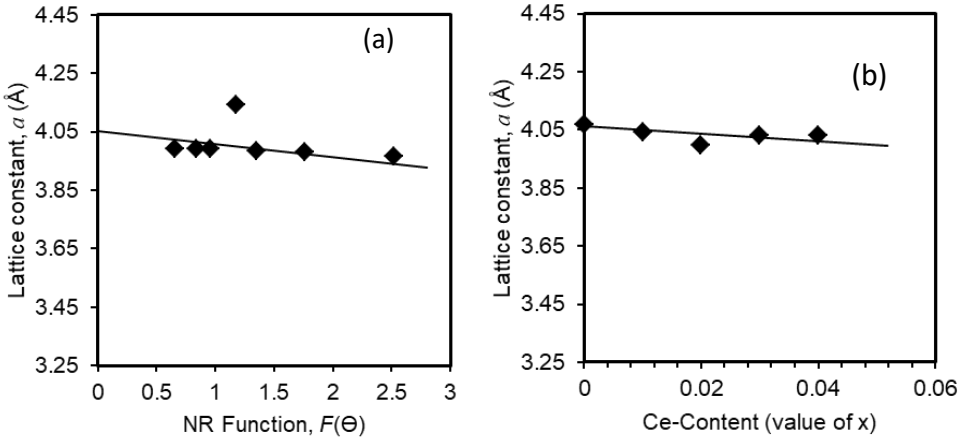

Fig. 2. (a) Representative curve showing the lattice constant vs Nelson-Riley function (here x = 0.00 in $Ba_{1-x}Ce_xTiO_3$) and (b) Lattice constant,*a* vs amount of Ce dopant.

Table 1. Lattice constants (*a*) and Particle sizes (D) of the samples of different compositions.

$Ba_{1-x}Ce_xTiO_3$	Lattice constant, *a* (Å)	Particle Size,D(nm)
x = 0.00	4.0685	34.40
x = 0.01	4.0465	33.03
x = 0.02	3.9977	31.76
x = 0.03	4.0313	30.59
x = 0.04	4.0301	29.51

It is observed that the particle size decreases with increasing Ce doping and X-ray density of the samples can be considered to be increases with Ce doping, because the dopant Ce has higher atomic mass (140.12) compared to Ba (137.33) [18].

3.2 Surface Morphology

The SEM micrographs of $BaTiO_3$ doped with Ce with different concentrations (sintered at 1200 °C) are shown in Figs. 3(a-e). From the SEM micrographs of the sintered pellets it is clear that grain distribution is uniform throughout the sample's surface, which suggests the compactness and homogeneity of the samples. The grains are generally circular in shape. As the amount of Ce increases the grain size also increases. In the images some shadows are observed, because the samples may not smoothly polished. These may arise due to the presence of some voids in the samples. But these void decreases with higher Ce dopant.

3.3 Frequency and Temperature Dependent Dielectric Constant

Fig. 4(a) shows the representative curves for the variation of ε' with frequency from 100 Hz to 100 kHz of the compositions measured at constant temperature. It is observed that as shown in Fig. 4(a) the value of ε' decreases rapidly with the increase in frequency below 1 kHz and it remains nearly constant at frequencies above 1 kHz. Fig. 4(b) shows the variation of ε' with frequency at different temperatures (–25 °C to 30 °C). The variations of ε' for different Ce doping concentrations at different temperatures are irregular. Though the changing pattern of ε' with below room temperature shows nearly similar, the ε' of all the samples remain very high, and

therefore are suitable for high frequency devices such as multilayer capacitors. The value of ε' is observed to increase at lower temperatures. It is observed that ε' for pure $BaTiO_3$ is lower than that of Ce doped $BaTiO_3$, and increases with Ce doping. The higher values of ε' observed at lower frequencies can be explained on the basis of space charge polarization due to inhomogeneous dielectric structure and sample's resistivity [19]. Though the change in ε' with the addition of dopant Ce is irregular, the decrease in ε' with the increase in Ce content indicates the space charge polarization in the samples. Our results are supported by the research reported in Refs. [20,21]. Yeasmin *et al.* also found that the value of ε' decreased with the increase in frequency and increased as the amount of dopant was increased [18].

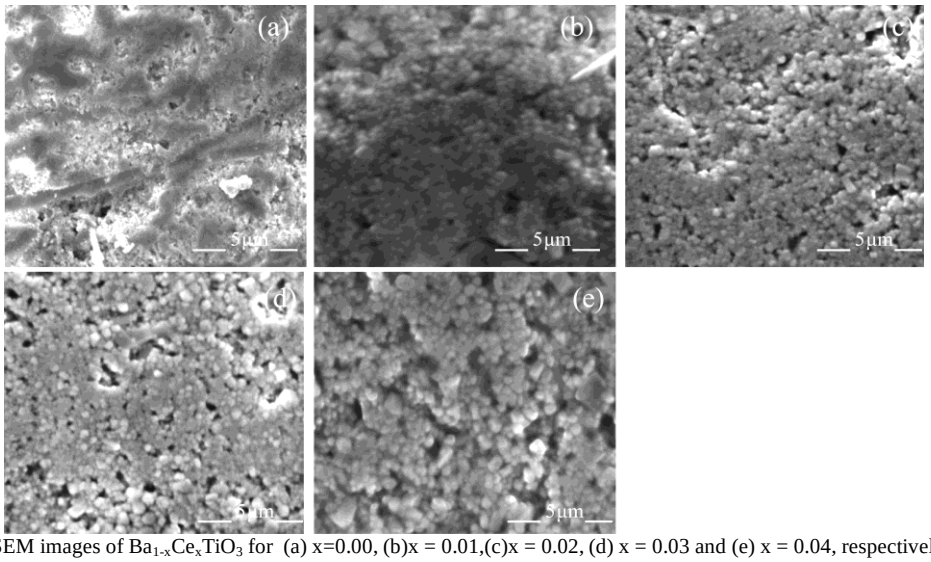

Fig.3. SEM images of $Ba_{1-x}Ce_xTiO_3$ for (a) x=0.00, (b)x = 0.01,(c)x = 0.02, (d) x = 0.03 and (e) x = 0.04, respectively.

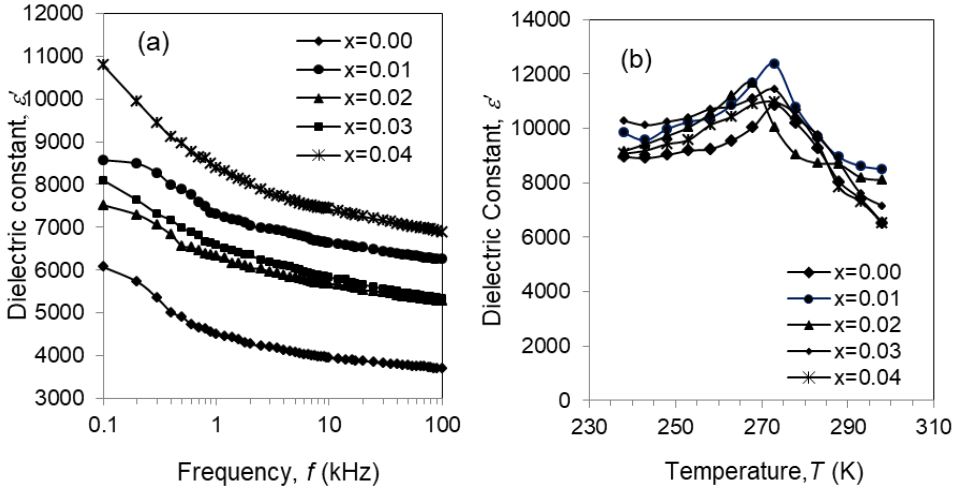

Fig. 4. The variation of the dielectric constant of $Ba_{1-x}Ce_xTiO_3$where x = 0.0, 0.01, 0.02, 0.03 and 0.04 compounds with (a) frequency at 303 K, (b) with temperature at frequency 50 kHz.

Table 2:Peak value of the dielectric constant (ε'_{max}) and the Curie temperature (T_c) for samples of different compositions at 100 kHz.

Value of x in $Ba_{1-x}Ce_xTiO_3$	ε'_{max}	T_c (K)
0.00	10550	273
0.01	12100	278
0.02	11985	277
0.03	10880	274
0.04	10210	272

Fig. 4 (b) shows the representative curves for the variation of the □□ at a constant frequency (50 kHz) of the composition $Ba_{1-x}Ce_xTiO_3$ (where x=0.0, 0.01, 0.02, 0.03, and 0.04) with temperature. The samples follow the rule of ferroelectrics that is the □□ increases with the rise in temperature up to a maximum value (ε'_{max}) and give a T_c where it undergoes a transition from orthorhombic phase to tetragonal phase in the intermediate temperature region (–25 °C to 30 °C) [2]. The ε'_{max} and T_c of the samples for different compositions at 100 kHz are presented in Table 2. It is observed that ε'_{max} increases with Ce doping as compared to that of undoped samples. Similar phenomena were observed by Yunov *et al.* [22]. The T_c of the samples initially increases, but decreases for further addition of dopant. Similar results was reported by Chen *et al.* [23] where they showed the dielectric behavior with temperature with different Bi doping in $Ba_{0.6}Sr_{0.4}TiO_3$ ceramics.

3.4 Frequency and Temperature Dependent Loss Tangent

The loss tangent is a parameter of a dielectric material that quantifies its inherent dissipation of electromagnetic energy. The dielectric losses are a combined result of alternating current electrical conduction and orientational polarization of the matter. Due to dipole relaxation and conductivity the energy losses occur in dielectrics. The portion of the energy of an alternating electrical field in a dielectric medium is converted into heat.

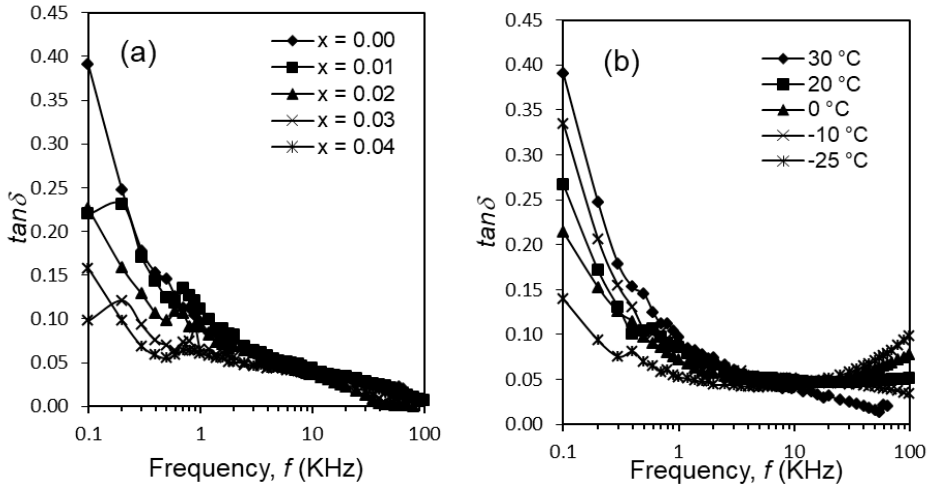

Fig. 5. Variation of the loss tangent of $Ba_{1-x}Ce_xTiO_3$ with frequency at (a) constant temperature (30 °C) and (b) different temperatures for a particular doping concentration (x = 0.00).

Therefore, the loss factor ($tan\delta$) of a dielectric is an indication of the energy loss as heat, which is calculated by using the relation

$$tan\delta = \frac{G_p}{2\pi fc} \quad \ldots \quad \ldots \quad \ldots \quad \ldots \quad \ldots \quad \ldots(3)$$

where, G_p is the conductance. The $tan\delta$ of the samples was calculated in the frequency range of 100 Hz to 100 kHz from the data taken below the room temperature. The variation of the $tan\delta$ of $Ba_{1-x}Ce_xTiO_3$ (x=0.00, 0.01, 0.02, 0.03 and 0.04) with frequency at constant temperature (30 °C) and at different temperatures at a particular doping concentration (x = 0.00) are presented in Figs. 5(a) and 5(b), respectively. $tan\delta$ shows a good agreement with the dielectric constant where it decreases with the increase in the doping concentration. At the lower frequency region the loss tangent decreases slightly but at the mid frequency remain nearly constant and again it tends to increase at higher frequency region. All the temperature shows almost same characteristics except at temperature below 0 °C.

3.5 AC Conductivity

Representative curves showing the frequency dependent *ac* conductivity at room temperature for the compounds sintered at 1200 °C with different concentration of Ce in $Ba_{1-x}Ce_xTiO_3$ and those at different temperature for a particular doping amount are shown in Figs. 5(a) and 5(b), respectively.

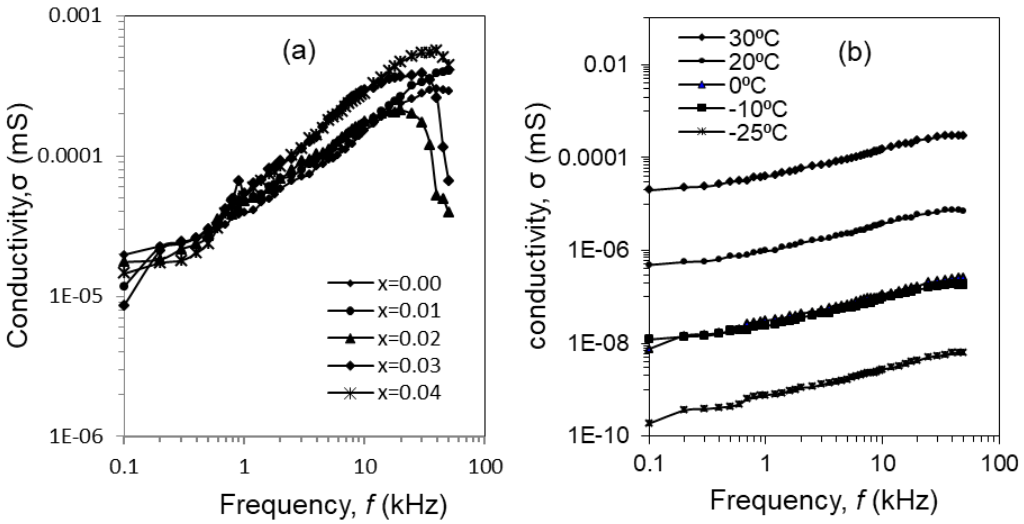

Fig. 6. Variation of the conductivity with frequency (a) at room temperature for $Ba_xCe_{1-x}TiO_3$samples, where x= 0.00,0.01,0.02,0.03, 0.04 and (b) at different temperatures for a particular doping concentration (x = 0.00).

From Fig. 5(a) it is clear that with the increase of frequency the conductivity increases and at a frequency of about 60 kHz the conductivity goes to its maximum value and then decreases with the increase in frequency. It is also observed that the conductivity increases almost exponentially with frequency. Similar phenomena are observed at temperature 20, 0, −10 and −25 °C, which are represented in Fig. 5(b). As the temperature decreases the value of ac conductivity also decreases. The ac conductivity is found of the order of 10^{-4} mS at room temperature and it decreases to the

order of 10^{-10} mS at –25 °C. Our results are in good agreement with the results obtained by Singh *et al.* [24].

5. CONCLUSIONS

The structural, dielectric and dielectric properties of the pure and Ce-doped $BaTiO_3$ ceramics were investigated through XRD, SEM analysis and *ac* electrical measurements. The variations ofdielectric constant, loss tangent and *ac* conductivity as a function of frequency were studied at the temperature range 30 to –25 °C. SEM analyses show that with the increase in Ce concentration the grain size of the samples increases, but their distribution were observed to be uniform throughout the surface suggesting the compactness and homogeneity of the samples. XRD pattern confirmed the single phase of the $Ba_{1-x}Ce_xTiO_3$. The position of the diffraction peaks does not change with the increase of Ce concentration, which indicates that the crystal structure remains unchanged, because as Ce has smaller ionic radii, its doping effect on the lattice constant does not change the crystal structure. The lattice constants were observed to decrease slightly with the increase in Ce dopant. The particle size it is observed to decrease with increasing Ce content. As there is an increase in lattice constant and the atomic mass of dopant Ce (140.12) is higher than Ba (137.33), density of the samples are considered to increase with Ce doping. The values of ε' are observed to decrease with frequency up to 1 kHz and then remain nearly constant for all temperatures. The ε' increases with temperature and undergoes a transition around 270 K. The variation of loss tangent with frequency of the compositions $Ba_{1-x}Ce_xTiO_3$ shows a decreasing trend with the increase in frequency. The *ac* conductivity increases almost in an exponential manner and reaches a peak value and then decreases. The frequency for this peak conductivity shifted towards lower frequency with the increase in Ce content.

ACKNOWLEDGEMENTS

The authors would like to acknowledge the supports of Mrs. Shireen Akter and Dr. Dilip Kumer Saha of Atomic Energy Centre, Dhaka during XRD measurements.

REFERENCES

[1] H. Thurnauer, Reflections Growth and decline of ceramics Engineering, Am. Ceram. Soc. Bull, **56**, 861-66 (1977).

[2] W. D. Kingery, H. K. Bowen, D. R. Uhlmann , Introduction to ceramics, John Wiley & Sons, 2nd edition(1975).

[3] H. F. Kay, W. J. Merz, Electrical behavior of barium titanate single crystal at low temperature" Phys. Rev. **76**, 1221(1949).

[4] S. Choudhury, S. Akter, M. J. Rahman, A. H. Bhuiyan, S. N. Rahman, N. Khatun, M. T. Hossain, Study of dielectric and electrical properties of zirconium doped barium titanate perovskite, J. Bangladesh Acad. Sci., **32**(2), 221-229 (2008).

[5] R. Islam, S. Choudhury, S. N. Rahman, M. J. Rahman, The effect of manganese doping on the grain size and transition temperature of barium titanate ceramics, J. Ceram. Process. Res., **13**(3), 248-251 (2012).

[6] M. Mostafa, M. J. Rahman, S. Choudhury, Enhanced Dielectric Properties of $BaTiO_3$ Ceramics with Cerium Doping, Manganese Doping and Ce-Mn Co-doping, Sci. Engin. Compos. Mater., **26**(1), 62-69 (2019).

[7] A. Kumari and B. D. Ghosh, La doped barium titanate/polyimide nanocomposites: A study of the effect of La doping and investigation on thermal, mechanical and high dielectric properties, J. Appl. Polym. Sci., **135**, Article ID: 46826, (2018).

[8] M. de A Gomes , L. G. Magalhães, A. R. Paschoal, Z. S. Macedo, Á. S. Lima, K. I. B. Eguiluz, and G. Ri. Salazar-Banda, An eco-friendly method of $BaTiO_3$ nanoparticle synthesis using coconut water, J. Nanomater. **2018**, Article ID 5167182, (2018).

[9] Y. Liua , X. Dengb, J. Chenc and Q. Zhou, Preparation and dielectric characterization of Ce-doped $BaTiO_3$ nanotubes, IOP Conf. Ser.: Mater. Sci. Eng., **381**, 012104 (2018).

[10] B.Jaffe,W.R.Cook and H.Jaffe,Peizoelectric, The antiferroelectric –ferroelectric phase transition in lead–containing and lead free perovskite, Ceramics,**3**,53-57(1971).

[11] D. Makovec, Z. Samardzija and D. Koler, Solid solubility of cerium in $BaTiO_3$, J. Solid Stat. Chem., **123**, 30 (1996).

[12] B. S. Saxena, R. C. Gupta and P. N. Saxena, Fundamental of solid state physics, Meerut, 10^{th} Edition(2003).

[13] G. Alart, and G. de, Microstructure and texture dependence of the dielectric anomalies and dc conductivity of Bi_3TiNbO_9 ferroelectric ceramics, J. Appl. Phys.,**97**, 1084103(2005).

[14] A. Yamaji and T. Murakami, Preparation, characterization and properties of Dy-doped small grained $BaTiO_3$ceramics, J. Am. Ceram. Soc., **60**, 97-101 (1977).

[15] Markalich and J. Lockhart, Sol-gel derived $Ba(Fe,Ti)O_3$ ferroelectric materials for infrared sensors, J. Am. Ceram. Soc.,**49**, 291(1966)

[16] B. Jaffe, W. R., Cook, Jr., H. Jaffe, Piezoelectric ceramics, Academic Press, London, (1971).

[17] S.-C. Jeon, B.-K. Yoon, K.-H. Kim, S.-J. L. Kang, Effects of core/shell volumetric ratio on the dielectric-temperature behavior of $BaTiO_3$, J. Adv. Ceram., **3**(1), 76–82 (2014).

[18] S. Yeasmin, S. Choudhury, M. A. Hakim, A. H. Bhuiyan and M. J. Rahman, Structural and dielectric properties of pure and cerium doped barium titanate, J. Ceram. Proces. Res., **12**,387-391(2011).

[19] S. Kumer, J. Kumar, Ac conductivity, dielectric losses, permittivity behavior of $Ba_xSr_{1-x}Fe_{0.8}Co_{0.2}O_{3-\delta}$(x=0, 0.5 and 1) Ceramics, Mater. Sci., **42**, 2105-2111(2007).

[20] S. K. Patri, R.N.P Choudhary, Electrical properties of $LaBi_8Fe_5Ti_3O_{27}$, J. Mater Sci., **19**, 1240-1246 (2008).

[21] D. Kaur, S. B. Narang, Electronic properties of complex barium-neodymium titanates in microwave regime. *In proc. Int. Conf. Emerging Tren. Comp. Electron. Engin. March 24-25*, Dubai, 26-28 (2012).

[22] O. I. V. Yunov, Plutenko, A.G. Belous, A. V. Bilous'ko, PTCR effect of solid solutions based on the (1-x)$BaTiO_{3-x}Na_{0.5}Bi_{0.5}TiO_3$ system, Chem. Met. Alloys, **3**,120-125(2010).

[23] W. Chen. X. Yao, X. Wei, Structural and dielectric properties of Bi doped $Ba_{0.6}Sr_{0.4}TiO_3$ ceramics, J. Mater. Sci., **43**, 1144-1150(2008).

[24] P. K. Singh, A. Chandra, The effect of ferroelectric ceramics materials $Ba_{0.70}Sr_{0.30}TiO_3$ and $Ba_{0.88}Sr_{0.12}TiO_3$, J. Phys. D.: Appl. Phys., **36**,193-196,(2003).